



Contents lists available at ScienceDirect



Catalysis Today

journal homepage: www.elsevier.com/locate/cattod

Ga-MCM-41 nanoparticles: Synthesis and application of versatile heterogeneous catalysts

Xavier Collard^a, Li Li^b, Warunee Lueangchaichaweng^b, Arnaud Bertrand^a, Carmela Aprile^{a,*}, Paolo P. Pescarmona^{b,**}

^a Unit of Nanomaterial Chemistry (CNano), University of Namur (UNAMUR), Department of Chemistry, Rue de Bruxelles 61, 5000 Namur, Belgium

^b Centre for Surface Chemistry and Catalysis, University of Leuven (KU Leuven), Kasteelpark Arenberg 23, 3001 Heverlee, Belgium

ARTICLE INFO

Article history:

Received 16 December 2013

Received in revised form 13 February 2014

Accepted 21 February 2014

Available online xxx

Keywords:

Ga-MCM-41

Nanoparticles

Heterogeneous catalyst

Glycerol

Lactate

Epoxidation

ABSTRACT

Ga-MCM-41 materials with nanosized particles (<150 nm) were prepared according to two new synthesis methods. The structural and textural properties of the materials were characterized by XRD, N₂-physisorption, TEM, SEM and EDX, while ⁷¹Ga MAS-NMR was employed to monitor the coordination of the gallium atoms. The two materials were tested as heterogeneous catalysts in three relevant reactions in the context of green production of valuable chemicals: (1) the reaction of glycerol with acetone to produce solketal; (2) the conversion of the triose sugar dihydroxyacetone to ethyl lactate; (3) the epoxidation of cyclooctene with aqueous hydrogen peroxide. The two nanosized Ga-MCM-41 materials show different catalytic behaviour in the various reactions, with the material prepared with lower Si/Ga displaying a higher versatility. This catalyst reaches higher turnover numbers compared to conventional Ga-MCM-41 reported in the literature. This result is ascribed to the higher specific surface area and to the shorter channels of the nanoparticles, which enhance the accessibility of the active sites.

© 2014 Elsevier B.V. All rights reserved.

1. Introduction

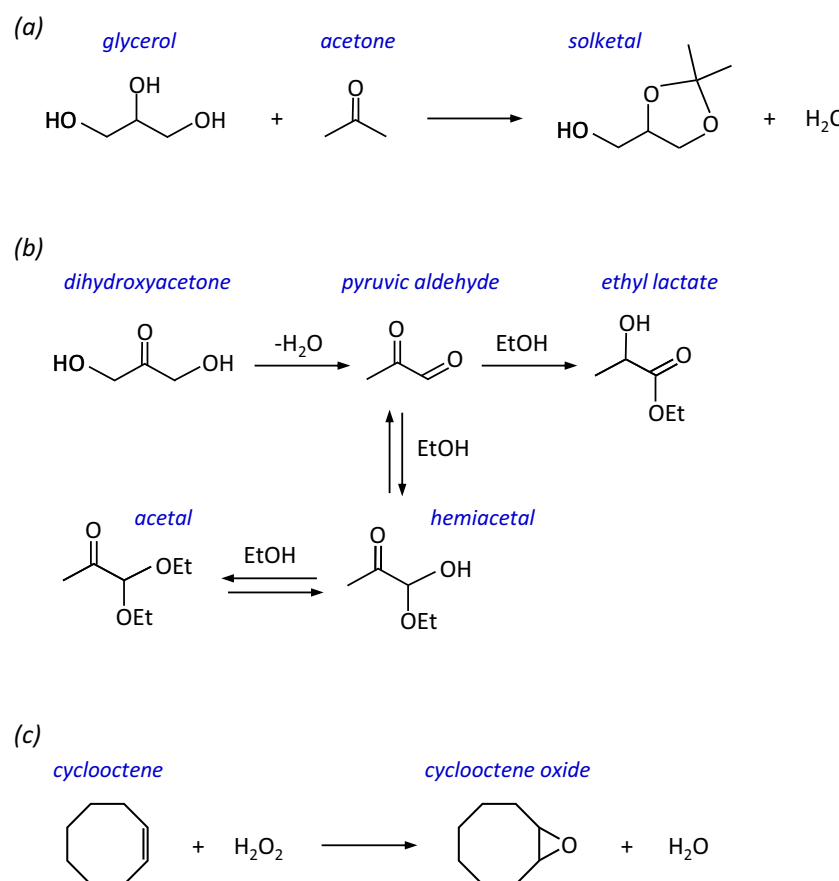
Heterogeneous catalysts are widely employed in the industrial production of a broad range of bulk and fine chemicals, as they can be readily separated from the reaction mixture and reused in consecutive cycles. The reaction occurs at the interface between the solid catalyst and the reactants, which can be in the liquid or in the gas phase. This represents the major limitation of heterogeneous compared to homogenous catalysts, the latter being typically more active due to a better contact between the reactants and the catalytic sites. Many research efforts have been dedicated to the improvement of the activity of heterogeneous catalysts by increasing their specific surface area, thus maximizing the number of accessible active sites per gram of material. Within this concept, a variety of approaches have been investigated, ranging from the reduction of the size of the catalyst particle to the nanoscale in order to increase their surface-to-volume ratio [1,2], to the synthesis of highly porous materials [3,4]. An important class of heterogeneous catalysts belonging to the last group is represented by

metal-substituted silicates, which can be prepared both in the form of microporous crystalline solids (zeolites) or as mesoporous materials (e.g. MCM-41, SBA-15, TUD-1) [3–6]. Zeolites in which metal atoms isomorphously substitute a fraction of the silicon atoms in the framework display well-defined and highly active single sites, but they often suffer from diffusion limitation of reactants and products due to the small size of the micropores. Generation of hierarchical zeolites through the creation of mesopores by desilication has been proposed as a possible way to overcome this issue [7]. Another widely studied approach to minimize diffusion limitations is based on the preparation of mesoporous metal-substituted silicates employing surfactants as structure directing agents. MCM-41 and SBA-15 are the best known materials of this family, both being characterized by a hexagonal array of parallel mesopores [4,5]. MCM-41 materials have been prepared using different metal atoms partially substituting silicon in their framework, thus enabling their application in a broad range of catalytic reactions [5]. In recent years, it has been demonstrated that the catalytic activity of Ti-MCM-41 in the epoxidation of alkenes can be improved by reducing the particle size of this material to the nanoscale [8]. The enhancement was attributed to the reduced length of the channels and to the increased surface area, which guarantee better accessibility to the catalytically active sites. Here, we present the synthesis of Ga-MCM-41 materials in the form of nanoparticles (<150 nm), and their use as heterogeneous catalysts in three relevant reactions

* Corresponding author. Tel.: +32 81 724514.

** Corresponding author. Tel.: +32 16 321592.

E-mail addresses: carmela.aprile@unamur.be (C. Aprile), paolo.pescarmona@biw.kuleuven.be (P.P. Pescarmona).



Scheme 1. The three test reactions used to evaluate the catalytic performance of the XS-Ga-MCM-41 materials: (a) acetalization of acetone with glycerol producing solketal; (b) conversion of dihydroxyacetone to ethyl lactate; (c) epoxidation of cyclooctene with hydrogen peroxide.

in the context of the sustainable production of useful chemicals (**Scheme 1**). The first two reactions employ renewable compounds, glycerol and the related dihydroxyacetone, as substrates to produce solketal and ethyl lactate, respectively. The conversion of glycerol to added-value products is receiving attention in connection to the growing interest for biodiesel as alternative to fossil fuels. The manufacturing of biodiesel is based on the transesterification of triglycerides obtained from natural lipids, and yields glycerol as the main co-product (approximately 10 wt% of the amount of biodiesel produced) [9]. Glycerol can be converted to solketal (2,2-dimethyl-1,3-dioxolane-4-methanol) by an acetalization reaction with acetone. Solketal can be considered a reversible derivative of glycerol in which two of the alcohol functions are protected, thus allowing the synthesis of mono-, di- and triglycerides with different chains. Moreover, solketal can find application as fuel additive [10]. The acetalization reaction is typically catalyzed by Brønsted acids, though metal-substituted mesoporous silicates displaying mainly Lewis acidity have also been reported as promising catalysts for this reaction [11,12]. Ga-MCM-41 has never been employed before as catalyst for this reaction but it is expected to show good activity due to its Brønsted acidity induced by Ga atoms substituting Si atoms in tetrahedral sites in the framework, and possibly to Lewis acidity that is associated to extra-framework Ga species that are generally present in this type of material. The second reaction in which the nanosized mesoporous gallosilicates were tested is the conversion of the triose sugar dihydroxyacetone, which can be obtained by partial oxidation of glycerol, to ethyl lactate [13–16]. This attractive product can be employed as green solvent, as precursor for the synthesis of polylactic acid and in various other applications in the food, pharmaceutical and cosmetic industry [17]. This reaction is catalyzed by a combination of

Brønsted and Lewis acidity, with the former promoting the dehydration of dihydroxyacetone to pyruvic aldehyde, and the latter catalyzing the rearrangement of this intermediate to ethyl lactate [15]. Conventional Ga-MCM-41 has been reported to be active in this reaction, though the selectivity towards ethyl lactate was not complete [18]. The third reaction that was studied in this work is the sustainable epoxidation of cyclooctene with the environmentally benign hydrogen peroxide as the oxidant. Epoxides are useful compounds finding industrial application in the production of fine chemicals [19,20]. Transition-metal-free heterogeneous catalysts based on Al and Ga have been reported to be active and selective catalysts for the epoxidation of various alkenes with aqueous H₂O₂ [21–25].

The versatility of the nanosized Ga-MCM-41 materials was demonstrated by their activity in the three selected reactions. Comparison with the catalytic performance of the previously reported conventional Ga-MCM-41 in the conversion of dihydroxyacetone to ethyl lactate and in the epoxidation of cyclooctene allowed to prove the assets of the shorter channels and enhanced surface area of the Ga-MCM-41 nanoparticles.

2. Experimental

2.1. Materials

The reagents employed in the synthesis of the Ga-MCM-41 nanoparticles were all purchased from Sigma-Aldrich and used without further purification: cetyltrimethylammonium bromide (CTAB, purity ≥99%), ammonium hydroxide solution (NH₄OH, 28.0%), sodium hydroxide (NaOH, purity ≥97%), absolute ethanol (EtOH, purity ≥99.5%), tetraethylorthosilicate (TEOS, purity

≥99.999%) and gallium nitrate hydrate ($\text{Ga}(\text{NO}_3)_3 \cdot x\text{H}_2\text{O}$, purity ≥99.9%).

2.2. Synthesis of the Ga-MCM-41 nanoparticles (XS-Ga-MCM-41)

Extra-small gallosilicate mesoporous materials (XS-Ga-MCM-41) were prepared according to two different procedures, each employing a different Ga content and a different base. The first method was developed by combining elements from reported protocols for the preparation of conventional Ga-MCM-41 [26,27], with tailored modifications to promote the formation of smaller particles (e.g. shorter reaction time). The second method was inspired by the diluted solution route reported for the synthesis of Ti-MCM-41 nanoparticles [8]. In both methods, CTAB was stirred in milli-Q deionized water at 800 rpm until full dissolution of the surfactant. Next, a basic solution (NaOH 2.0 M or NH₄OH 28%) was added slowly, and the resulting solution was stirred for 30 min. $\text{Ga}(\text{NO}_3)_3$, previously dissolved in 1.0 mL of absolute ethanol, and TEOS were added separately to the solution in a dropwise manner. The molar composition of the synthesis mixture of the sample with higher Ga content (XS-Ga-MCM-41-H) was, 1 TEOS: 0.0625 $\text{Ga}(\text{NO}_3)_3$: 69 NH₄OH: 0.125 CTAB: 1.43 EtOH: 525 H₂O. The molar composition of the synthesis mixture of the sample with lower Ga content (XS-Ga-MCM-41-L) was 1 TEOS: 0.0241 $\text{Ga}(\text{NO}_3)_3$: 0.33 NaOH: 0.125 CTAB: 0.90 EtOH: 1212 H₂O. In both cases, the solution was stirred for 2 h at room temperature and subsequently subjected to a thermal treatment at 70 °C for 3 h. After filtration, the solid was washed three times with milli-Q water and ethanol (alternately) and dried at 60 °C for 16 h. Finally, the powder was calcined at 550 °C (heating rate of 4 °C min⁻¹) for 5 h under N₂ and 5 h in air.

A sample of XS-Ga-MCM-41-L was subjected to an ion-exchange treatment in order to replace the Na⁺ ions by H⁺. 1.0 g of XS-Ga-MCM-41-L was added to 20 mL of a 3.0 M aqueous solution of NH₄OH. The suspension was stirred for 5 h at room temperature to allow exchange of Na⁺ by NH₄⁺. After the exchange, the solid was removed by filtration and washed three times with absolute ethanol and water. Then, the sample was dried at 100 °C for 12 h and calcined at 550 °C to obtain the H⁺-form of the material, which was labelled XS-Ga-MCM-41-L (ion exchanged).

2.3. Characterization of the XS-Ga-MCM-41 materials

Powder X-ray diffraction (XRD) patterns were measured on a PANalytical X'pert pro diffractometer with Cu K α radiation ($\lambda = 1.54178 \text{ \AA}$). Specific surface area and porosity of the solids were determined from the nitrogen adsorption–desorption isotherms obtained at -196 °C with a volumetric adsorption analyzer (Micromeritics Tristar 3000). The samples were pre-treated at 150 °C for 24 h under a reduced pressure of 10⁻⁴ bar. The Brunauer–Emmet–Teller (BET) method was used to calculate the specific surface areas [28]. The Barrett–Joyner–Halenda (BJH) method applied to the adsorption isotherm was used to determine the pore size distributions [29]. Transmission electron microscopy (TEM) images were recorded on a Philips Tecnai 10 with an accelerating voltage of 80 kV. Field emission scanning electron microscopy (FE-SEM) images were obtained on a JEOL JSM 7500 instrument. Chemical compositions were determined by energy-dispersion X-ray spectroscopy (EDX) using an acceleration potential of 7.5 kV, and a working distance of 8 mm. ²⁹Si and ⁷¹Ga magic-angle spinning nuclear magnetic resonance (MAS-NMR) spectra were measured on a VARIAN 400 and a Bruker 500 spectrometer, respectively. The Si environment was studied at the resonance frequency of ²⁹Si (79.46 MHz). The samples were packed in a 4 mm zirconia rotor and measured with a spinning frequency of 8000 Hz. 4.14×10^6 scans were accumulated with a recycle delay of 6 s and a pulse length of 2.0 μs (30°). Tetramethylsilane (TMS)

was used as shift reference. The study of the Ga coordination was performed at the resonance frequency of ⁷¹Ga (152.52 MHz). The samples were packed in a 3.2 mm Chemagnetics rotor and measured with a spinning frequency of 12,000 Hz. 5×10^6 scans were accumulated with a recycle delay of 0.1 s and a pulse length of 1.2 μs (10°). The acid properties of XS-Ga-MCM-41-H were investigated by adsorption and temperature programmed desorption (TPD) of pyridine monitored by Fourier Transform infrared spectroscopy (FTIR). A self-supporting wafer of the sample (about 15 mg) was initially dried under vacuum at 400 °C for 1 h, and then cooled down to 50 °C in an in-house built vacuum infrared cell with ZnSe windows. Reference spectra were recorded at 350, 250, 150 and 50 °C. Next, the wafer was saturated with about 25 mbar of pyridine vapour at 50 °C for 10 min and then evacuated again for 30 min to completely remove physisorbed pyridine. Finally, the sample containing chemisorbed pyridine was subjected to TPD at 150, 250 and 350 °C for 30 min, with a heating rate of 4 °C min⁻¹. The IR spectra were recorded *in situ* at each of these temperatures. The amounts of acid sites were determined from the integral intensity of characteristic bands (1450 cm⁻¹ for Lewis acid sites, and 1545 cm⁻¹ for Brønsted acid sites) using Emeis molar extinction coefficients [30].

2.4. Catalytic tests

For the reaction of glycerol with acetone, the reaction mixture contained: 0.921 g of highly purified glycerol (purity 99%, 10 mmol), 0.581 g of acetone (10 mmol), 0.132 g of dioxane (1.5 mmol, as GC internal standard), and 1.48 g of *tert*-butanol (20 mmol, as solvent). 25 mg of catalyst was loaded at room temperature and the mixture was stirred and heated to 80 °C for 6 h. The catalytic tests were carried out in a 50-well reaction block, under vigorous stirring (1000 rpm) [31]. At the end of the reaction, the catalyst was separated by centrifugation and the reaction solution was analyzed by gas chromatography on a Trace GC Ultra from Interscience equipped with a polar column (PH POR-Q column, FT-3, 10 m, 0.25 mm) [12]. Recyclability tests were performed by centrifuging the sample at the end of the catalytic test, after which the reaction solution was removed. Then, the catalyst was washed with *tert*-butanol for five times. Afterwards, the solid was dried overnight at 100 °C and reused in a new catalytic run. Before the last reuse, the catalyst was calcined at 500 °C for 2 h (heating rate of 2 °C min⁻¹). Leaching tests were performed under the same reaction conditions employed for the catalytic tests (*vide supra*). The catalyst was removed from the reaction mixture after 30 min by centrifugation, followed by hot filtration at the same temperature of the catalytic test using a plastic syringe equipped with a 25 mm HPLC syringe filter from Altech, with a pore size of 0.2 μm . The filtrate was allowed to react for another 5 h 30 min. The reaction mixture was analyzed by GC both after 30 min and at the end of the filtrate test (6 h).

For the conversion of dihydroxyacetone (DHA) to ethyl lactate, 0.180 g of DHA (2 mmol, in the form of 1,3-dihydroxyacetone dimer) and 0.0215 g of decane (0.15 mmol, as GC internal standard) were dissolved in 3.92 g of ethanol (as solvent and reactant) at 45 °C for 30 min. Next, 50 mg of catalyst were added to the solution at room temperature. The reaction mixture was heated to 90 °C for 6 h under vigorous stirring (1200 rpm). The tests were carried out in the same 50-well reaction block used for the reaction of glycerol with acetone. At the end of the test, the catalyst was separated by centrifugation and the reaction solution was analyzed by gas chromatography (GC) on a Trace GC Ultra from Interscience equipped with an RTX-5 fused silica column (5 m; 0.1 mm). Recyclability tests were performed by separating the catalyst from the reaction mixture by centrifugation followed by washing with ethanol (five times). Next, the catalyst was dried overnight at 100 °C and reused in a new catalytic run. Before the last reuse, the catalysts were calcined at 500 °C for 2 h (heating rate of 2 °C min⁻¹). The leaching tests

were carried out with the same protocol employed for the reaction of glycerol with acetone (*vide supra*).

For the epoxidation reactions, 50 mg of the selected XS-Ga-MCM-41 were weighed in a glass vial. Then, a solution containing *cis*-cyclooctene (2.5 mmol), di-n-butyl ether (1.25 mmol, as GC internal standard) and 2.5 g of solvent (mixture of ethyl acetate and toluene, 1:1 in mass) was added into the vial, followed by addition of a 50 wt% aqueous solution of hydrogen peroxide (25 mmol H₂O₂). The solutions were dispensed using an automated high-throughput liquid-handling workstation (Tecan Genesis RSP 100) [31]. Then, the vials were capped, placed in an in-house developed 60-well reaction block [31], and stirred at 800 rpm and 80 °C for 22 h. Samples of the reaction solution were taken and analyzed after 1, 2, 4 and 22 h. The conversion and product yields were determined by gas chromatography (GC) on a Finnigan Trace GC Ultra from Interscience, equipped with an RTX-5 fused silica column (5 m; 0.1 mm).

3. Results and discussion

Mesoporous Ga-MCM-41 samples with extra-small particle size (XS-Ga-MCM-41) were synthesized and studied as heterogeneous catalysts for three relevant reactions: the acetalization of acetone with glycerol yielding solketal, the conversion of dihydroxyacetone to ethyl lactate, and the epoxidation of cyclooctene with hydrogen peroxide. The reduced particle size of the mesoporous solids is expected to lead to improved catalytic activity compared to conventional Ga-MCM-41 consisting of larger particles [32], due to increased accessibility to the active sites originating from the shorter channels and the higher specific surface area [8]. Two different synthesis protocols were used for preparing the materials: a standard method for the synthesis of Ga-MCM-41 modified by reducing the reaction time (entry 1 in Table 1) [26] and a diluted solution route adapted from a reported method for the preparation of Ti-MCM-41 nanoparticles (entry 2 in Table 1) [8]. In both cases, Ga(NO₃)₃ was employed as the metal source. The diluted solution route should enable the preparation of MCM-41 nanoparticles with a size distribution below 200 nm, while the modifications of the standard synthesis method for Ga-MCM-41 aim at defining an alternative synthesis procedure for preparing MCM-41 nanoparticles.

The physicochemical properties of the materials were investigated by a combination of different techniques. Small-angle X-ray diffraction analysis of the material with higher Ga content (XS-Ga-MCM-41-H) reveals the typical pattern of an MCM-41 architecture with an intense d_{100} peak at $2\theta = 2.4^\circ$ and two less defined signals corresponding to d_{110} and d_{200} reflections (Fig. 1a). This pattern is associated to the presence of a hexagonal array of cylindrical pores [33]. On the other hand, the material with lower Ga content (XS-Ga-MCM-41-L) displays only a main reflection, suggesting the presence of mesopores with a defined size but with a lower long-range ordering (Fig. 1b). For both materials, the wide-angle part of the XRD patterns did not display any peak, indicating the absence of any crystalline Ga₂O₃ phase [34], which could have formed if segregation of Ga species occurred during the synthesis. However, this does not allow excluding the presence of amorphous gallium oxide species, which could be present in the form of small, extra-framework clusters (*vide infra*).

N₂-physisorption measurements on XS-Ga-MCM-41-H revealed the typical type-IV isotherm of MCM-41 mesoporous materials, with a sharp inflection at low relative pressure characteristic of capillary condensation and corresponding to a very narrow mesopore size distribution centred at 2.3 nm (Fig. 2a and Table 1). Despite the high gallium loading, this sample displays an elevated specific surface area, close to 1000 m² g⁻¹. XS-Ga-MCM-41-L has slightly lower but still high surface area (869 m² g⁻¹).

The N₂-physisorption isotherms of XS-Ga-MCM-41-L also display an inflection at low relative pressure, though less pronounced, and present a clear hysteresis loop at higher relative pressure indicating the presence of a second type of porosity, attributed to interparticle voids (Fig. 2b). As a consequence, the pore size distribution of this material displays a narrow peak centred at 2.3 nm as for XS-Ga-MCM-41-H, but also a broad band between 15 and 45 nm. The presence of these large interparticle pores explains the higher total pore volume observed for XS-Ga-MCM-41-L. In order to distinguish the contribution of the internal mesopores from that of the interparticle voids, the pore volume was recalculated by excluding the contribution from the larger pores (corresponding to $p/p_0 = 0.8–1.0$) (Table 1). The resulting value gives an estimation of the internal mesopore volume, which follows the same trend as the surface areas of the two materials. This can be explained considering that the large interparticle voids are related to the external surface area of the particles, which typically represents a small fraction of the total surface area in mesoporous materials like MCM-41.

Transmission electron microscopy reveals that both XS-Ga-MCM-41 materials consist of small, irregular particles (Fig. 3a and b), in contrast with previous reports in which MCM-41 nanoparticles were shown to be approximately spherical [8]. The desired nanosized particles were obtained with both methods, with significantly smaller particles and narrower size distribution for XS-Ga-MCM-41-L (20–70 nm, compared to 20–150 nm for XS-Ga-MCM-41-H). The size difference is attributed to the employed synthesis conditions and suggests that the diluted solution route is more suitable to generate smaller nanoparticles. Moreover, in the case of XS-Ga-MCM-41-L some zones of condensation between the different particles are present (see inset of Fig. 3b). This observation is in agreement with the presence of the interparticle voids suggested by the N₂-physisorption analysis (*vide supra*). TEM images with higher magnification show that the hexagonal organization and parallel channels typical of MCM-41 are observed in many small domains in XS-Ga-MCM-41-H (Fig. 3c and d), while zones with less ordered, worm-like mesopores (though still with the same size) are also present. Highly ordered domains are scarcer in XS-Ga-MCM-41-L (Fig. 3b), in line with the less defined XRD pattern and N₂-physisorption isotherms measured for this sample (*vide supra*). These results suggest that the small scale of these particles can prevent the formation of an extensive hexagonal array of parallel channels. SEM investigation performed on both materials highlights the presence of a three-dimensional morphology and allows excluding the existence of flat surfaces (Fig. 3e and f). The transparency of the materials under the electron beam can be ascribed to the extra-small dimension of the solids. A screening of the two materials by energy dispersive X-ray spectroscopy mapping (performed by SEM) reveals a homogeneous distribution of gallium in the two samples with no formation of large (*i.e.* >50 nm) separate domains of gallium oxide species (Fig. S1 in the Supporting Information).

Ideally, the synthesis of mesoporous gallosilicates should involve the incorporation of Ga as a single site in tetrahedral coordination within the silica framework. The gallium coordination was studied by solid state ⁷¹Ga MAS-NMR (Fig. 4). XS-Ga-MCM-41-H presents two signals at *ca.* –10 and 150 ppm that can be assigned to octahedral extra-framework species and to Ga in tetrahedral coordination, respectively [35,36]. The integrated areas of the two peaks are very similar, which implies a similar fraction of intra- and extra-framework gallium. Conversely, the spectrum of XS-Ga-MCM-41-L shows a single, intense peak at 150 ppm, indicating that gallium is prevalently present in tetrahedral coordination. This trend is in agreement with previous reports that showed that the incorporation of gallium in framework tetrahedral sites is more efficient at low metal loading [35]. The degree of condensation leading to the

Table 1

Physicochemical properties of the XS-Ga-MCM-41 materials.

Entry	Sample	Si/Ga ratio		Temperature and duration of the synthesis	BET surface area [$\text{m}^2 \text{g}^{-1}$]	Average pore size [nm]	Pore volume [$\text{cm}^3 \text{g}^{-1}$]	Internal pore volume [$\text{cm}^3 \text{g}^{-1}$] ^b
		In the reaction mixture	In the final material ^a					
1	XS-Ga-MCM-41-H	16	15	2 h RT + 3 h 70 °C	976	2.3	1.15	0.72
2	XS-Ga-MCM-41-L	41	44	2 h RT + 3 h 70 °C	869	2.3	1.62	0.54

^a Data determined by EDX.^b Data calculated for p/p_0 from 0.0 to 0.8.

formation of Si–O–Si bonds was monitored by ^{29}Si MAS NMR spectroscopy. The ^{29}Si NMR spectrum of XS-Ga-MCM41-H (Fig. S2 in the Supporting Information) displays a combination of Q³, Q⁴ signals with a Q⁴/Q³ ratio of 1.15. The elevate contribution of Q³ species is attributed to the small size of the particles, which is expected to lead to a high concentration of surface silanol groups.

The two XS-Ga-MCM-41 materials present both small particles and high surface area, which are promising features for catalytic

application in the selected test reactions, while the number and type of acid sites is expected to be different in the two materials. The presence of gallium isomorphously substituting silicon in tetrahedral sites within the silica framework generates Brønsted acid sites if H⁺ are the counter ions that balance the charge difference between Si and Ga. In general, not all gallium is introduced in the framework of Ga-MCM-41, and the extra-framework species can generate Lewis acidity [37]. Based on the ^{71}Ga NMR

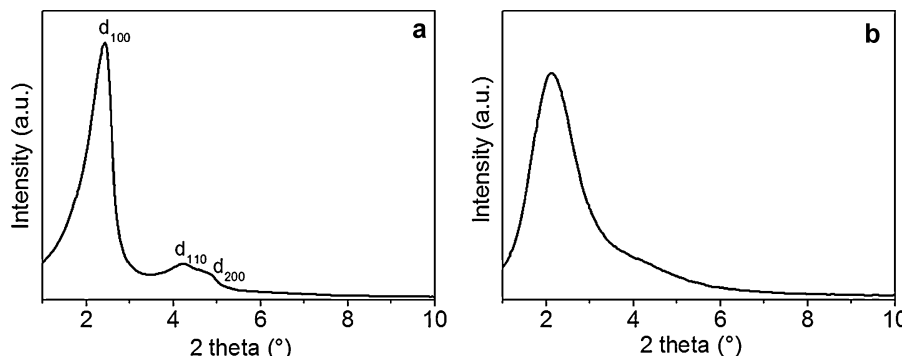


Fig. 1. XRD patterns of XS-Ga-MCM-41-H (a) and -L (b) in the small-angle region ($2\theta = 1\text{--}10^\circ$). The d_{100} values calculated from these XRD patterns using Bragg's law are in the typical range for MCM-41 materials ($d_{100} = 3.7 \text{ nm}$ for XS-Ga-MCM-41-H and $d_{100} = 3.9 \text{ nm}$ for XS-Ga-MCM-41-L) [8].

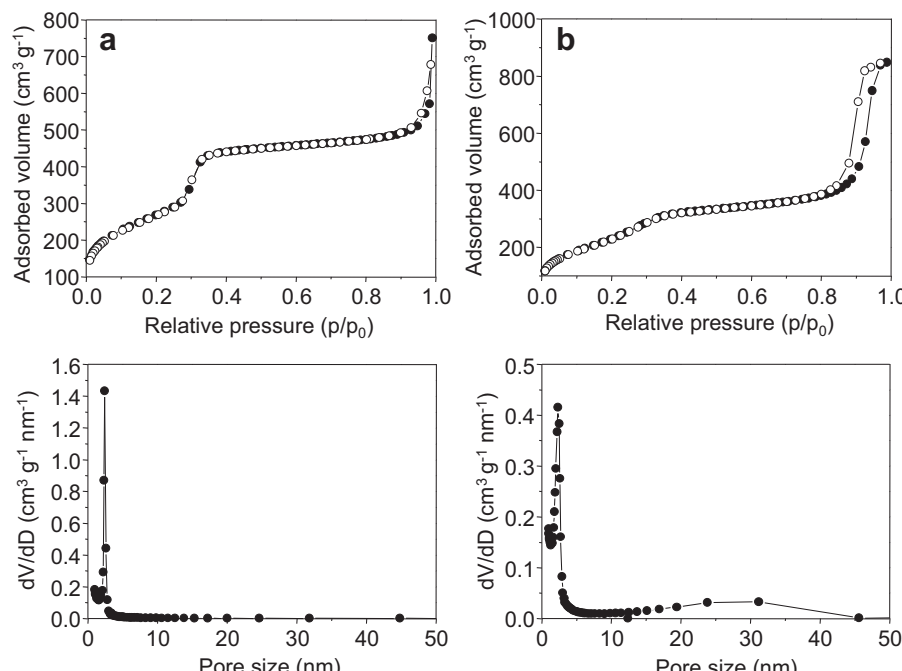


Fig. 2. N₂-physisorption isotherms (top) and pore size distribution (bottom) of XS-Ga-MCM-41-H (a) and -L (b).

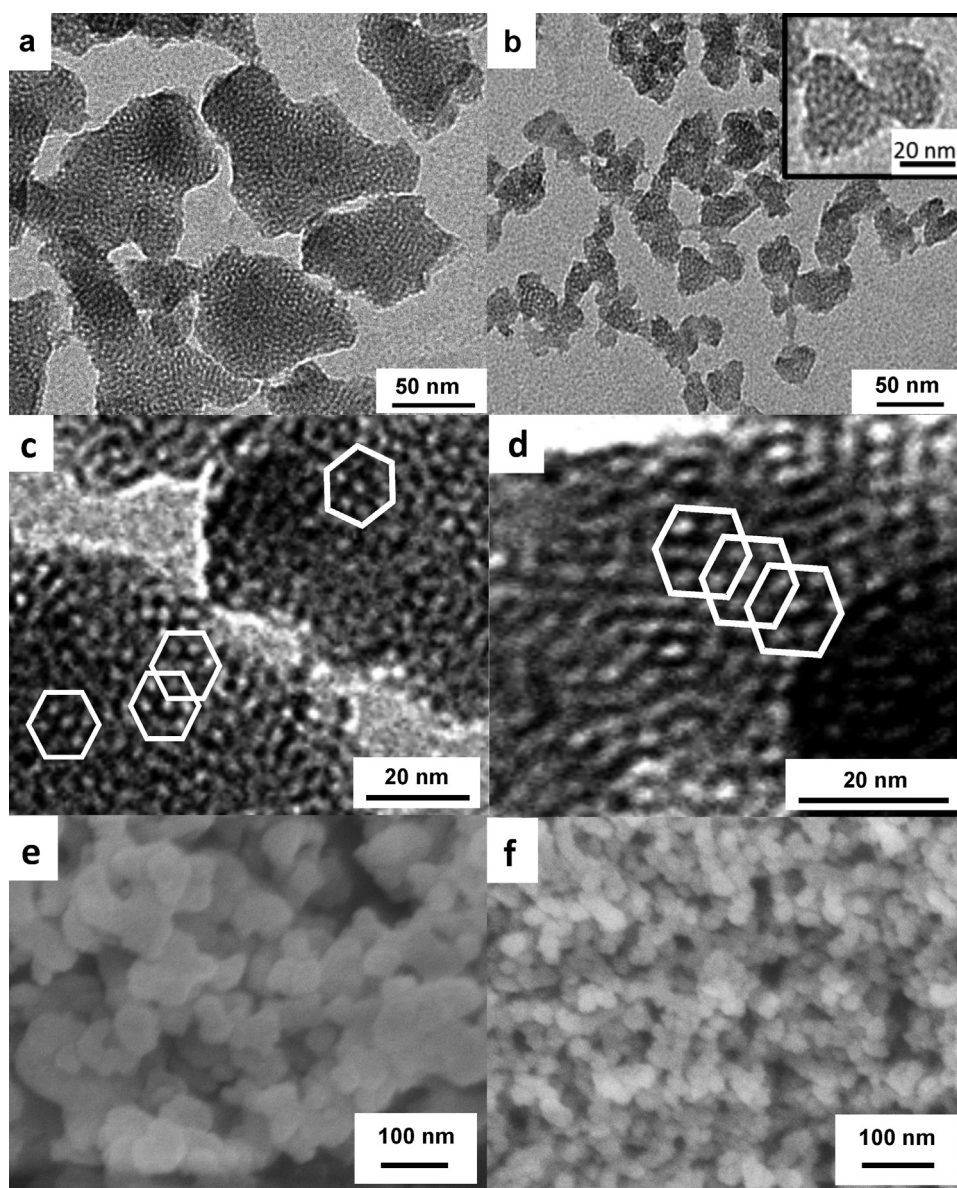


Fig. 3. TEM and SEM images of XS-Ga-MCM-41-H (TEM: a, c, d; SEM: e) and XS-Ga-MCM-41-L (TEM: b; SEM: f).

spectra, XS-Ga-MCM-41-L should mainly present Brønsted acid sites, while XS-Ga-MCM-41-H also contains a relevant fraction of octahedral extra-framework gallium species and, therefore, is expected to display both Brønsted and Lewis acidity. These differences are reflected in the catalytic behaviour of the two materials.

The tests were performed with relatively low catalyst loading at which only moderate conversions are expected, in order to detect clearly the differences in activity between the two materials. In the reaction of glycerol with acetone to yield solketal, the two catalysts achieve a very similar degree of conversion, which corresponds to

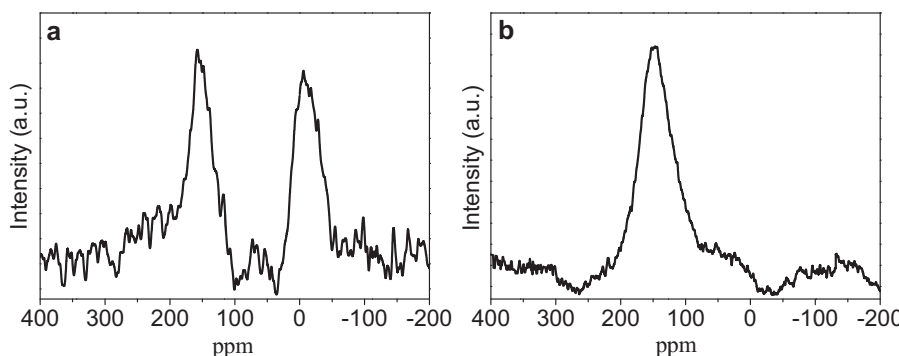


Fig. 4. Solid state ^{71}Ga NMR spectra of XS-Ga-MCM-41-H (a) and -L (b).

Table 2

Catalytic performance of the XS-Ga-MCM-41 materials in the reaction of glycerol with acetone to produce solketal.

	$X_{\text{glycerol}} (\%)$	$S_{\text{solketal}} (\%)$	TON
XS-Ga-MCM-41-H	28	>99	125
XS-Ga-MCM-41-L	25	>99	361

Conditions: 25 mg of catalyst, glycerol (10 mmol), acetone (10 mmol), dioxane (1.5 mmol), *tert*-butanol (1.48 g), 6 h at 80 °C. Turnover number is defined as TON = mol_{glycerol converted}/mol_{Ga}.

a much higher turnover number for the material with the lowest gallium content, XS-Ga-MCM-41-L (Table 2). Complete selectivity towards the five-membered-ring solketal was observed in both cases [12]. On the other hand, the conversion of dihydroxyacetone to ethyl lactate proceeded much more efficiently over XS-Ga-MCM-41-H in terms of lactate yield, turnover number and selectivity towards the desired lactate product (Table 3). These results can be understood by taking into account the mechanism of the two reactions. In the conversion of dihydroxyacetone to ethyl lactate, Brønsted acid sites catalyze the dehydration of the triose sugar to pyruvic aldehyde, while Lewis acid sites are required for the rearrangement of this intermediate to the desired lactate product. In the absence of Lewis acid sites and if the Brønsted acid sites are sufficiently strong, the products of the acetalization of pyruvic aldehyde, *i.e.* its hemiacetal and acetal, would be obtained instead (Scheme 1) [15–18]. This is the case of the reaction over XS-Ga-MCM-41-L, thus confirming the Brønsted acid nature of this catalyst. XS-Ga-MCM-41-H was anticipated to display both Lewis and Brønsted acidity: accordingly, it achieves a much higher lactate yield and selectivity. Notably, the turnover number obtained with this catalyst is much higher compared to that of a previously reported conventional Ga-MCM-41 (TON = 2.2), with the same Si/Ga ratio and tested under similar conditions [18]. On the other hand, the conversion of glycerol to solketal is not only determined by the total amount of acid sites of the catalyst, but is also favoured by a relatively high hydrophobicity of the catalyst surface, which would help removal of the water side-product (Scheme 1), thus minimizing the reverse reaction (*i.e.* the hydrolysis of solketal) [11,12]. It is known that the hydrophobicity of zeolitic aluminosilicates increases with the Si/Al ratio [3]. Therefore, the higher turnover number observed for XS-Ga-MCM-41-L in the synthesis of solketal is ascribed to its higher Si/Ga ratio compared to XS-Ga-MCM-41-H, and to its Brønsted acid sites, which are well established active sites for this acetalization reaction [11,12].

The results of the first two catalytic tests and of analysis by ⁷¹Ga NMR strongly suggested that XS-Ga-MCM-41-H should contain both Lewis and Brønsted acidity. In order to test this hypothesis, the acid properties of XS-Ga-MCM-41-H were evaluated by adsorption and temperature programmed desorption (TPD) of pyridine monitored by FT-IR spectroscopy (Fig. 5). The material displays the anticipated combination of Lewis and Brønsted acid sites, with a moderately larger population of the former under the employed experimental conditions (L/B = 1.4 at 150 °C).

The reusability of XS-Ga-MCM-41-H was assessed in the reaction of glycerol with acetone and in the conversion of dihydroxyacetone to ethyl lactate (Fig. 6). In line with previous reports on other heterogeneous catalysts for these reactions, the activity

Lewis acid sites [mmol g ⁻¹]		Brønsted acid sites [mmol g ⁻¹]		L/B ratio	
150°C	250°C	150°C	250°C	150°C	250°C
0.092	0.011	0.068	0.003	1.4	3.4

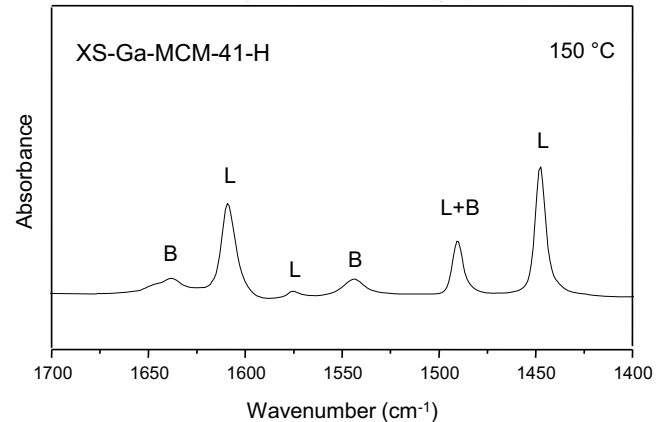


Fig. 5. FT-IR spectrum of pyridine adsorbed at 150 °C over XS-Ga-MCM-41-H, and type and amount of surface acid sites.

gradually decreases upon reuse if the catalyst is only washed with the reaction solvent and dried between two consecutive cycles [12,18]. This behaviour has been ascribed to the adsorption of organic species on the surface of the catalyst, which cannot be efficiently removed by washing procedures. Accordingly, the activity can be restored after thermal treatment of the catalyst at 500 °C (5th catalytic cycle). The heterogeneous nature of the catalyst was investigated by hot filtration leaching tests. For both reactions, only a minor increase in conversion in the filtrate solution was observed after separation of the catalyst (probably due to the unavoidable permeation of some of the small catalyst particles through the filter) [12,18], confirming that the observed activity originates from the heterogeneous material.

The third reaction in which the XS-Ga-MCM-41 materials were tested as catalysts is the epoxidation of cyclooctene with the environmentally benign aqueous hydrogen peroxide as the oxidant. In previous work, conventional Ga-MCM-41 was reported to be the most active catalyst for this reaction among a set of microporous and mesoporous alumino- and gallosilicates [24,38]. The performance of Ga-MCM-41 was optimized by carrying out the reaction in a mixture of ethyl acetate and toluene as solvent and by working with an excess of hydrogen peroxide relative to the alkene (10:1). Similar reaction conditions were used in this work to test the epoxidation activity of the XS-Ga-MCM-41 materials, though significantly lower catalyst loadings relative to the alkene were employed. Both XS-Ga-MCM-41 samples are active in the epoxidation of cyclooctene and display full selectivity towards the epoxide product (Table 4). Coordinatively unsaturated extra-framework Ga-sites and framework tetrahedral Ga-OH have been proposed to act as catalytic sites by activating hydrogen peroxide for the epoxidation reaction [39]. In line with its lower Si/Ga ratio, XS-Ga-MCM-41-H leads to higher epoxide yields at all reaction stages, reaching almost

Table 3

Catalytic performance of the XS-Ga-MCM-41 materials in the conversion of dihydroxyacetone to ethyl lactate.

	$Y_{\text{lactate}} (\%)$	$Y_{\text{acetal}} (\%)$	$Y_{\text{hemiacetal}} (\%)$	$S_{\text{lactate}} (\%)$	TON
XS-Ga-MCM-41-H	12	3	5	60	8.9
XS-Ga-MCM-41-L	0	3	0	0	4.3

Conditions: 50 mg of catalyst, dihydroxyacetone (2 mmol), decane (0.15 mmol), ethanol (3.92 g), 6 h, 90 °C. Turnover number is defined as TON = mol_{DHA converted}/mol_{Ga} (the mol of DHA converted are calculated as the sum of the mol of the observed reaction products).

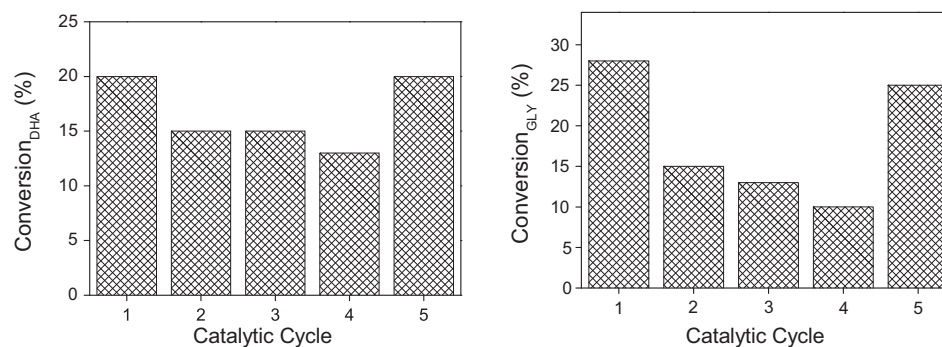


Fig. 6. Recycling experiments performed with the XS-Ga-MCM-41-H catalyst for the conversion of dihydroxyacetone (left) and glycerol (right). After the 4th cycle the catalyst was calcined at 500 °C.

Table 4

Catalytic performance of the XS-Ga-MCM-41 materials in the epoxidation of cyclooctene with hydrogen peroxide.

	4 h			22 h	
	Y _{epoxide} (%)	S _{epoxide} (%)	TON	Y _{epoxide} (%)	S _{epoxide} (%)
XS-Ga-MCM-41-H	9.5	>99	4.8	91	>99
XS-Ga-MCM-41-L	6.7	>99	9.2	49	>99
XS-Ga-MCM-41-L (ion-exchanged)	7.2	>99	9.9	80	>99

Conditions: 50 mg of catalyst, *cis*-cyclooctene (2.5 mmol), di-n-butyl ether (1.25 mmol), aqueous H₂O₂ (50 wt%, 25 mmol), 2.5 g of a 1:1 mixture of ethyl acetate and toluene, 80 °C. Turnover number is defined as TON = mol_{alkene converted}/mol_{Ga}.

full conversion of the alkene into the epoxide after 22 h of reaction (Fig. 7). On the other hand, XS-Ga-MCM-41-L is superior in terms of turnover number, in line with the results observed in the reaction of glycerol with acetone (*vide supra*). Notably, both XS-Ga-MCM-41 catalysts display improved turnover number compared to previously reported conventional Ga-MCM-41 (Si/Ga = 15, TON = 2.4 after 4 h of reaction at 80 °C) [38], confirming the advantages of the nanosized Ga-MCM-41 materials originating from their higher surface area and shorter channels. EDX showed that XS-Ga-MCM-41-L, which was synthesized using NaOH as base, contains a relevant amount of residual sodium (Ga/Na = 2.6). Previous reports on Ga-MCM-41 showed that exchange of Na⁺ with H⁺ leads to an increase of the catalytic activity of the material, in agreement with the catalytic role of surface Ga-OH sites [24]. Therefore, XS-Ga-MCM-41-L was treated with NH₄OH in order to exchange Na⁺ for NH₄⁺, followed by a thermal treatment to convert NH₄⁺ into H⁺. The virtually complete removal of sodium was confirmed by EDX measurements. As expected, the ion-exchanged catalyst displays improved activity, reaching much higher epoxide yield after 22 h of reaction compared to the as-synthesized XS-Ga-MCM-41-L (Fig. 7 and Table 4).

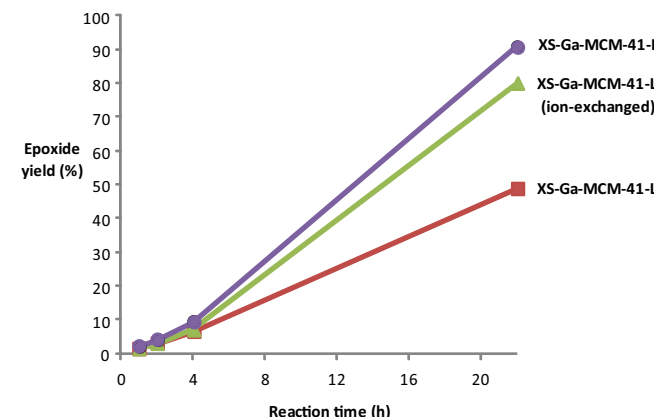


Fig. 7. Epoxidation of cyclooctene with aqueous H₂O₂ over XS-Ga-MCM-41 catalysts.

4. Conclusions

Two novel mesoporous gallosilicates with extra-small particle size (XS-Ga-MCM-41) were synthesized using protocols characterized by a very short reaction time and mild thermal treatment. Both materials consist of nanosized, irregular particles and display a remarkably high surface area and a pore size distribution typical of mesoporous MCM-41-like materials. The XS-Ga-MCM-41 materials were tested as catalysts in three relevant reactions: the synthesis of solketal from glycerol and acetone, the synthesis of ethyl lactate from dihydroxyacetone and the epoxidation of cyclooctene with the environmentally friendly H₂O₂ as the oxidant. The more versatile of the two catalysts is active in all three reactions and displays higher turnover numbers when compared to conventional Ga-MCM-41 with the same Si/Ga ratio. This result is attributed to the higher specific surface area and shorter channels of the nanosized material, which lead to more accessible active sites. Recycling tests demonstrated that the catalyst can be used in multiple catalytic runs without substantial decrease in catalytic performance when regenerated by thermal treatment. The physicochemical features of the XS-Ga-MCM-41 catalysts together with the straightforward synthetic approach make these materials attractive for other catalytic applications.

Acknowledgement

The authors acknowledge sponsoring in the frame of a START1 research program (STRT1/10/035).

Appendix A. Supplementary data

Supplementary data associated with this article can be found, in the online version, at <http://dx.doi.org/10.1016/j.cattod.2014.02.055>.

References

- [1] N.R. Shiju, V.V. Gulants, Appl. Catal. A-Gen. 356 (2009) 1–17.

- [2] X. Sheng, B. Wouters, T. Breugelmans, A. Hubin, I.F.J. Vankelecom, P.P. Pescarmona, *Appl. Catal. B* 147 (2014) 330–339.
- [3] Introduction to zeolite science and practice, in: H. van Bekkum, E.M. Flanigen, P.A. Jacobs, J.C. Jansen (Eds.), *Stud. Surf. Sci. Catal.*, vol. 137, 2nd ed., Elsevier, Amsterdam, 2001.
- [4] A. Corma, *Chem. Rev.* 97 (1997) 2373–2419.
- [5] A. Taguchi, F. Schüth, *Micropor. Mesopor. Mater.* 77 (2005) 1–45.
- [6] S. Telalovic, A. Ramanathan, G. Mul, U. Hanefeld, *J. Mater. Chem.* 20 (2010) 642–658.
- [7] D. Verboekend, J. Pérez-Ramírez, *Catal. Sci. Technol.* 1 (2011) 879–890.
- [8] (a) K.F. Lin, P.P. Pescarmona, H. Vandepitte, D.D. Liang, G. Van Tendeloo, P.A. Jacobs, *J. Catal.* 254 (2008) 64–70;
(b) K.F. Lin, P.P. Pescarmona, K. Houthoofd, D.D. Liang, G. Van Tendeloo, P.A. Jacobs, *J. Catal.* 263 (2009) 75–82.
- [9] F. Ma, M.A. Hanna, *Biore sour. Technol.* 70 (1999) 1–15.
- [10] A. Sokolowski, A. Piasecki, B. Burczyk, *J. Am. Oil Chem. Soc.* 69 (1992) 633–638.
- [11] (a) J. Deutsch, A. Martin, H. Lieske, *J. Catal.* 245 (2007) 428–435;
(b) C.X.A. da Silva, V.L.C. Goncalves, C.J.A. Mota, *Green Chem.* 11 (2009) 38–41.
- [12] L. Li, T.I. Koranyi, B.F. Sels, P.P. Pescarmona, *Green Chem.* 14 (2012) 1611–1619.
- [13] Y. Hayashi, Y. Sasaki, *Chem. Commun.* 21 (2005) 2716–2718.
- [14] R.M. West, M.S. Holm, S. Saravananurugan, J. Xiong, Z. Beversdorf, E. Taarning, C.H. Christensen, *J. Catal.* 269 (2010) 122–130.
- [15] P.P. Pescarmona, K.P.F. Janssen, C. Delaet, C. Stroobants, K. Houthoofd, A. Philip-paerts, C. De Jonghe, J.S. Paul, P.A. Jacobs, B.F. Sels, *Green Chem.* 12 (2010) 1083–1089.
- [16] C.B. Rasrendra, B.A. Fachri, I. Gusti, B.N. Makertihartha, S. Adisasmitho, H.J. Heeres, *ChemSusChem* 4 (2011) 768–777.
- [17] M. Dusselier, P. Van Wouwe, A. Dewaele, E. Makshina, B.F. Sels, *Energy Environ. Sci.* 6 (2013) 1415–1442.
- [18] L. Li, C. Stroobants, K. Lin, P.A. Jacobs, B.F. Sels, P.P. Percarmona, *Green Chem.* 13 (2011) 1175–1181.
- [19] S.T. Oyama, *Mechanisms in Homogeneous and Heterogeneous Epoxidation Catalysis*, Elsevier Science, 2008.
- [20] F. Cavani, J.H. Teles, *ChemSusChem* 2 (2009) 508–534.
- [21] D. Mandelli, M.C.A. van Vliet, R.A. Sheldon, U. Schuchardt, *Appl. Catal. A-Gen.* 219 (2001) 209–213.
- [22] R. Rinaldi, U. Schuchardt, *J. Catal.* 227 (2004) 109–116.
- [23] P.P. Pescarmona, K.P.F. Janssen, P.A. Jacobs, *Chem. Eur. J.* 13 (2007) 6562–6572.
- [24] P.P. Pescarmona, J. Van Noyen, P.A. Jacobs, *J. Catal.* 251 (2007) 307–314.
- [25] C. Aprile, E. Gobechiya, J.A. Martens, P.P. Pescarmona, *Chem. Commun.* 46 (2010) 7712–7714.
- [26] G.T. Palomino, J.J.C. Pascual, M.R. Delgado, J.B. Parra, C.O. Areán, *Mater. Chem. Phys.* 85 (2004) 145–150.
- [27] Q. Cai, W.-Y. Lin, F.-S. Xiao, W.-Q. Pang, X.-H. Chen, B.-S. Zou, *Micropor. Mesopor. Mater.* 32 (1999) 1–15.
- [28] B.C. Lippens, J.H. de Boer, *J. Catal.* 4 (1965) 319–323.
- [29] E.P. Barret, L.G. Joyner, P.P. Halenda, *J. Am. Chem. Soc.* 73 (1951) 373–380.
- [30] C.A. Emeis, *J. Catal.* 141 (1993) 347–354.
- [31] W. Lueangchaichaweng, I. Geukens, A. Peeters, B. Jarry, F. Launay, J.L. Bonardet, P.A. Jacobs, P.P. Pescarmona, *Comb. Chem. High Throughput Screen.* 15 (2012) 140–151.
- [32] M. Chatterjee, T. Iwasaki, Y. Onodera, T. Nagase, H. Hayashi, T. Ebina, *Chem. Mater.* 12 (2000) 1654–1659.
- [33] U. Ciesla, F. Schüth, *Micropor. Mesopor. Mater.* 27 (1999) 131–149.
- [34] M. Rodríguez-Delgado, C.O. Areán, *Mater. Lett.* 57 (2003) 2292.
- [35] C.-F. Cheng, H. He, W. Zhou, J. Klinowski, J.A. Sousa Gonçalves, L.F. Gladden, *J. Phys. Chem.* 100 (1996) 390–396.
- [36] D.J. Kim, C.-H. Shin, S.B. Hong, *Micropor. Mesopor. Mater.* 83 (2005) 319–325.
- [37] H. Kosslick, G. Lischke, G. Walther, W. Storek, A. Martin, R. Fricke, *Micropor. Mater.* 9 (1997) 13–33.
- [38] P.P. Pescarmona, P.A. Jacobs, *Catal. Today* 137 (2008) 52–60.
- [39] W. Lueangchaichaweng, N.R. Brooks, S. Fiorilli, E. Gobechiya, K. Lin, L. Li, S. Parres-Escalapez, E. Javon, S. Bals, G. Van Tendeloo, J.A. Martens, C.E.A. Kirschhock, P.A. Jacobs, P.P. Pescarmona, *Angew. Chem. Int. Ed.* 53 (2014) 1585–1589.